Crossover transition in flowing granular chains

Xialing Ulrich,[1] Eliot Fried,[2] and Amy Q. Shen[3]

[1]*Department of Mechanical, Aerospace & Structural Engineering, Washington University in St. Louis, St. Louis, Missouri 63130, USA*
[2]*Department of Mechanical Engineering, McGill University, Montréal, Quebec, Canada H3A 2K6*
[3]*Department of Mechanical Engineering, University of Washington, Seattle, Washington 98195, USA*

We report on the dynamical and statistical behavior of flowing collections of granular chains confined two-dimensionally (2D) within a rotating tumbler. Experiments are conducted with systems of chains of fixed length, but various lengths are considered. The dynamics are punctuated by cascades of chains along a free-surface cascades, which drive the development of mixed porous/laminar packing arrangements in bulk. We investigate the conformation of the system, as characterized by the porosity of the flow region occupied by the chains and the mean-square end-to-end distance of the chains during flow. Both of these measures show crossover transitions from a 2D self-avoiding walk to a 2D random walk when the chain length becomes long enough to allow self-contact.

PACS number(s): 45.70.Vn, 45.70.Qj, 05.40.−a

A system of macroscopic granular chains is a special type of granular medium which is interesting not only in its own right but also because many analogous microscopic systems, such as polymers or DNA in suspension, are collections of chainlike objects. The flow dynamics and nonequilibrium behavior of systems of macroscopic granular chains might help elucidate important problems in the crystallization of soft matter and the formation of localized structures in materials consisting of macromolecules, such as gels. Recent studies of granular chains have focused mainly on single chains subject to external forcing. For example, knotting and unknotting of vertically vibrated chains [1,2], the entropic tightening of a figure-8 chain [3], and the formation of spiral shapes in a chain on a vibrating plate have been reported [4]. Belmonte *et al.* [5] investigated the dynamics, such as emphasizing knotting and unknotting, of an excited hanging chain. Recently, Kudrolli *et al.* [6] reported the swarming and swirling behavior in self-propelled granular rods that showed local ordering and aggregation at the sidewalls. Prentis and Sisan [7] studied the conformations of a thermally excited polymer by placing a granular chain on a 2D surface among randomly moving (and colliding) ping pong balls. The mean-square end-to-end distance of the chain was found to follow a power-law behavior with respect to the number of links with exponent that of a 2D self-avoiding random walk (SAW).

There are, of course, many statistical mechanical models of chainlike polymers [8], with the SAW and conventional random walk (RW) the most studied and capturing many important macroscopic features of polymers in solution [9]. For a single polymer chain consisting a n freely jointed beads with $N=n-1$ links, the SAW model shows that the mean-square end-to-end distance $\langle r^2 \rangle$ satisfies $\langle r^2 \rangle \sim N^{2\nu}$, with exponent ν equal to 1, 0.75, and 0.588 for the one-dimensional (1D), two-dimensional (2D), and three-dimensional (3D) cases, respectively [10–13]. The universal critical exponent ν of a RW is given by $\nu=0.5$ independent of dimension [10,14]. However, many experiments studying single real polymers in ideal solutions yield a critical exponent [10,14]. $\nu \sim 0.59$ independent of the type of molecule and solution. Furthermore, Maier *et al.* [15] and Valle *et al.* [16] performed experiments on single DNA chains and ob-

tained $\nu \sim 0.79$ and $\nu \sim 0.59$ for the 2D and 3D cases, respectively. Due to excluded volume effects, the SAW model provides a better description for actual polymers.

In this work, we report results concerning the dynamical and statistical behavior of collections of granular chains rotated in a 2D cylindrical tumbler. We observe a variety of complex spatiotemporal patterns. The nature of these patterns depends on chain length, the filling percentage of the chains inside the tumbler, and the rotation rate of the tumbler. To characterize the global statistical state of the system, we focus on the average packing porosity of the granular chains under flow, the chain conformations, and the mean-square end-to-end distance of single chains. The porosity displays a jump at the minimum bead number required to form a loop in a single chain. The statistical behavior of a randomly selected chain during flow follows a crossover transition between a 2D SAW and a 2D RW behavior.

The granular chains used in our experiments are hollow steel spheres of diameter 0.208 cm coupled by steel rods of diameter 0.0508 cm (McMaster Carr). The rods act as rigid bonds that rotate freely and allow maximum distances of 0.286 cm between each pair of beads. It takes $n=9$ beads to form the smallest closed loop of a chain [Fig. 3(e)]. The chains are cut to specified lengths consisting of n beads ($n=2,5,8,9,10,12,15,20,25,30,50$). A large number of chains with fixed n are placed within a 19.05 cm diameter tumbler of gap size of 0.254 cm, enabling quasi-2D motions of the enclosed chains. The tumbler is made of transparent acrylic plates and is free to rotate about an axis oriented perpendicular to gravity. The inner surfaces of the tumbler are acrylic and are not treated before use. The radial boundary of the tumbler is aluminum.

The n-bead chains are initially laid within the tumbler layer by layer with minimum spacing [Fig. 1(a)]. The filling percentage η is defined as the ratio of area occupied by the chains to the surface area of the inner surface of the tumbler. Initial values of η considered are 20%, 40%, and 60%. The tumbler is mounted on an axle (Fig. 1) and rotated by a motor at a specified constant rotation rate ω. For each n and η, the tumbler is rotated at varying speeds, while instantaneous chain conformations, packing porosities, and mean-square end-to-end distances are recorded.
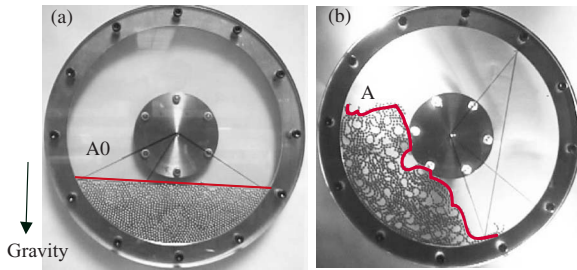
FIG. 1. (Color online) (a) A close-packed collection of ten-bead chains with an initial filling percentage of 40%. (b) A snapshot at rotation rate of 0.1 rev/s. Red lines show the contour of the free surface of the ten-bead chains.

The flow dynamics result from gravity pulling the chains downwards, frictional interactions with the walls of the rotating tumbler, chain-chain interactions, and bead-bead interactions. Our study focuses on flow regimes with small rotation rates. Centrifugal forces are therefore negligible in comparison to gravitational and frictional forces. With rotation of the tumbler, chains are pulled upwards to the tumbler until the topmost chains lose stability and fall down the free surface. The initially flat free surface also roughens substantially [Fig. 1(a)], showing an S-like profile similar to those seen in conventional particulate flows [17,18]. For sufficiently small rotation rates, a discrete avalanching regime, also familiar from particulate flows [17,18], is observed. As the rotation rate increases, a continuous flow regime emerges in which the chains close to the radial boundary of the tumbler exhibit a solid-body rotation while the chains close to the flow surface tend to extend and become more mobile. As falling chains arrive at the radial boundary of the tumbler they are dragged up anew to the free surface of the flow, creating a continuous cycle (see [19]). Since the flow is 2D, chains cannot entangle but rather slide in parallel as laminar layers.

The conformations of a single chain dyed red (for easy visualization) have also been tracked (see Fig. 2) and a continuous spectrum of shapes has been observed. The chains tend to stretch out before tumbling [Fig. 2(a)]. As a single chain falls along the free surface, its shape changes, becoming more compact [Fig. 2(b)]. As the same chain rises from the bottom below the free surface, its shape almost remains unchanged. Hence, the granular chains system exhibits more fluidlike behavior near the free surface and more solidlike behavior close to the radial boundary of the tumbler (see [19]). The shape of a single granular chain formed at each cycle appears random but the closed loop configuration can only occur for $n \geq 9$, in which case the closed loop configuration tends to be stable during flow (see [19]).

This prevalence of looped structures increases the porosity of the "solid" bulk part of the flow as the loops create voids that are difficult for other chains to penetrate. We have investigated the dependence of porosity upon n, η, and ω, defining the porosity as $p=1-A_0/A$, where A_0 is the initial area occupied by the chains and A is the area occupied by the chains during flow (Fig. 1). Figure 3 shows the dependence of p upon η (panel a) and granular Froude number that is related to ω, L (panel b) for chains of varying length. Here, $Fr=\omega^2 L/g$, with L as the maximum contour length of the chain when it is fully extended.
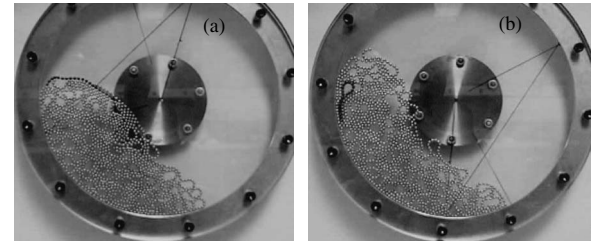

FIG. 2. A system of 20-bead chains arising from an initial filling percentage of 40%, with rotation rate of 0.05 rev/s. Image (a) shows a snapshot of a dyed chain on the free surface. Image (b) shows the same dyed chain forming a loop after moving from the free surface and being dragged up from the radial boundary of the tumbler.

For $\eta=20\%$ and $\omega=0.1$ rev/s, the average packing porosity p_n for $n=2$, 5, 8, 9, 20, 30, and 50 takes values of $p_2=0.125$, $p_5=0.176$, $p_8=0.178$, $p_9=0.351$, $p_{20}=0.393$, $p_{30}=0.395$, and $p_{50}=0.353$. Thus, p_n doubles with a jump at $n \sim 9$ [Fig. 3(a)]. This result is made evident in Figs. 3(c) and 3(d), which show that for fixed filling percentage η and rotation rate ω, the expansion is more pronounced for longer chains. The jump also coincides with the minimum number $n=9$ of beads required to form a closed loop. Due to stick-slip motion, the chains fall from the top due to gravity and organize themselves layer by layer by lamination and create spacings among chains. When $n<9$, voids can only be formed by the spacing between chains. When $n \geq 9$, the average porosity consists of the contribution from the loops and the spacing between parallel chains, leading to an increase in p. This argument can be supported by the following estimate. Consider an ideal situation where all chains ($n \geq 9$) form loops and the spacing between chains does not change as the chain length increases. If each nine-bead chain forms a loop
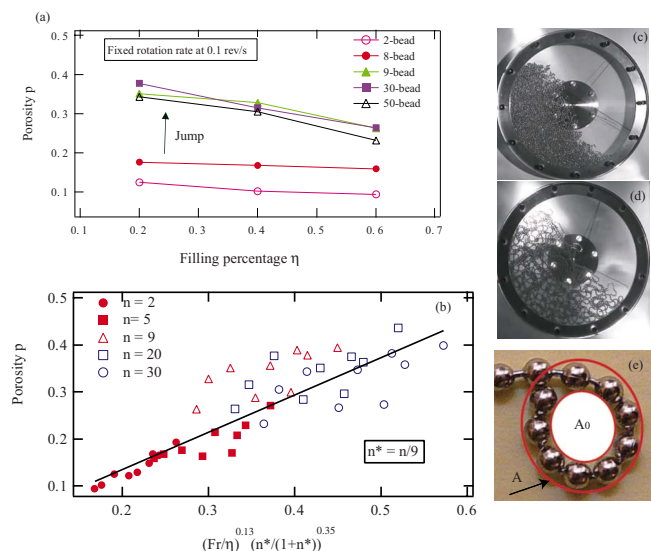

FIG. 3. (Color online) (a) For a fixed rotation rate ω, average porosity p versus filling percentage η with varying chain length n. (b) Porosity p versus dimensionless number $(Fr/\eta)^{0.13}[n^*/(1+n^*)]^{0.35}$ while varying chain length, filling percentage, and rotation rate. The solid black line is the best linear fit. For an filling percentage of 40% and rotation rate of 0.1 rev/s, (c) two-bead chains. (d) 30-bead chains. (e) Estimate of $p_{loop}=1-A_0/A$.

during flow, then for a tumbler filled to 20% of its capacity with nine-bead chains $p_{\text{loop}}=0.271$ [Fig. 3(e)]. For $n>9$, the values of p differ by at most 11% and agree well with the estimate $p \approx p_2 + p_{\text{loop}}$. This is consistent with the observation that, for chains long enough to form loops, the smallest possible loop size occurs with the highest probability.

From Fig. 3(a), we also observe that the average porosity $p=1-A_0/A$ decreases with increasing η for longer chains. This suggests that, when A exceeds half the available area, the curvature of the radial boundary of the tumbler might constrain the available range of chain conformations, increasing the area occupied by the chains. In Fig. 3(b), we also show how porosity varies with the granular Froude number (Fr=$\omega^2 L/g$, with L as the maximum contour length of the chain when it is fully extended), η, and $n^*=n/9$, n is the bead number. The solid black line is the linear fit from the data. It indicates that for chains with n beads, p increases with increasing rotation rate.

A statistical characterization of a system of granular chains under flow is provided by the mean-square end-to-end distance of the chains. For simplicity, we fix the filling percentage η at 20%, and for each chain length n between 5 and 50 (N between 4 and 49) we vary the rotation rate ω of the tumbler from 0.05 to 0.2 rev/s. We measure $\langle r^2 \rangle = \tau^{-1} \int_0^\tau r^2(t)dt$ for two (randomly selected) chains that are dyed red and blue. The end-to-end distance r of these two chains is acquired over a period of $\tau=20$ min and analyzed for 200 frames total. The observation time τ is sufficiently long to ensure that the time average of $\langle r^2 \rangle$ is independent of τ. For fixed flow conditions, the values of $\langle r^2 \rangle$ for the red and blue chains are consistent for each n considered. For $n \leq 9$, the standard deviation of $\langle r^2 \rangle$ varies from 0.039 to 0.16 cm^2 [see Fig. 4(a) of $\langle r^2 \rangle$ versus $N=n-1$]. For a fixed chain length, randomly selected red and blue chains yield very similar results, with rotation rates varying from 0.05 to 0.2 rev/s. This implies that $\langle r^2 \rangle$ is independent of rotation rate for short chains. However, for $n>9$, $\langle r^2 \rangle$ is sensitive to the rotation rate of the tumbler and has standard deviation between 0.17 and 1.6 cm^2. Moreover, it takes longer for $\langle r^2 \rangle$ to converge to its mean value for longer chains. This is consistent with the observation that longer chains have more conformational options. Observing Fig. 4(a), we also notice that for $N=49$, the measured values of $\langle r^2 \rangle$ are below the $\nu=0.5$ RW line. Since the chain length at $N=49$ is comparable to the tumbler diameter, the boundary effects tend to lower the average $\langle r^2 \rangle$ values, as the edge prevents the chain from fully extending. Even though $\langle r^2 \rangle$ does not fall perfectly on the $\nu=0.5$ line for longer chains, Fig. 4(a) does exhibit a crossover transition from shorter to longer chains. Experimental errors generally preclude the possibility that data point lie perfectly on the RW line.

For each flow condition (with fixed initial filling percentage $\eta=20\%$), we plot the mean-square end-to-end distance $\langle r^2 \rangle$ normalized by the square L^2 of the maximum contour length L, against the number $N=n-1$ of links [Fig. 4(b)]. The maximum contour length L is the length of a granular chain when it is completely extended and depends linearly on N. For $n \leq 9$, the data follow a power-law trend with $\langle r^2 \rangle/L^2 \sim N^{-0.5}$, while for $n>9$ the data follow a power-law trend with $\langle r^2 \rangle/L^2 \sim N^{-1}$. Since $L \sim N$, the best curve fitting
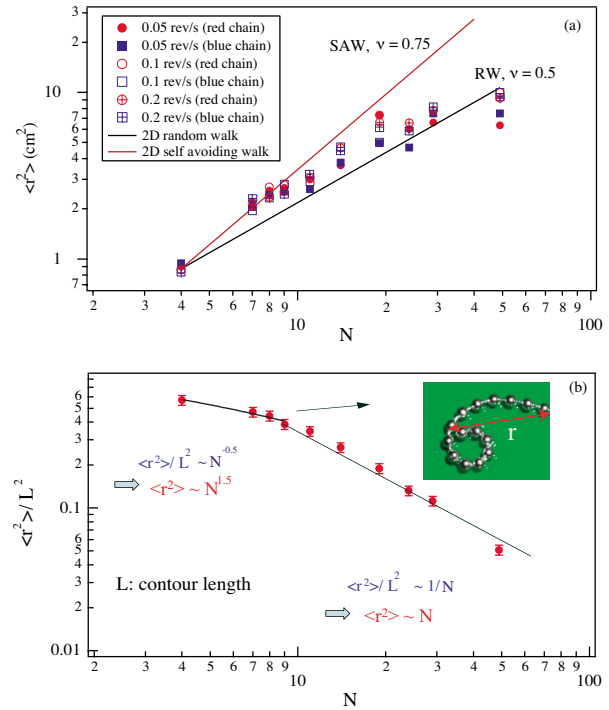

FIG. 4. (Color online) For $N=4,7,8,9,11,14,19,24,29,49$, (a) $\langle r^2 \rangle$ is plotted against the number of links for both red and blue chains at different rotation rates, $\omega=0.05$ rev/s (close symbols), $\omega=0.1$ rev/s (open symbols), and $\omega=0.2$ rev/s (cross symbols). (b) Mean-square end-to-end distance $\langle r^2 \rangle$ normalized by the maximum contour length square L^2 versus the number N of links.

in Fig. 4(b) leads to $\langle r^2 \rangle \sim N^{1.5}$ for $n \leq 9$ and $\langle r^2 \rangle \sim N$ for $n>9$. Recall that for the scaling law $\langle r^2 \rangle \sim N^{2\nu}$ between $\langle r^2 \rangle$ for a solution of polymer chains with N links $\nu \sim 0.5$ corresponds to 2D random walk while $\nu \sim 0.75$ corresponds to a 2D self-avoiding walk [20]. Figure 4 displays a crossover transition around $n=9$, i.e., shorter chains follow SAW statistics while longer chains follow the RW statistics. A plot of the average end-to-end distance $\langle r \rangle$ shows a similar transition at $n=9$. Due to space limitations, such a plot is not included here.

Since, for the chains used in our experiments, it takes $n=9$ beads to form the smallest possible loop in a granular chain, for chains with fewer than 9 beads, the beads on each single chain cannot touch and the chain has a higher probability to be in a fully close to extended configuration, meaning that motions of granular chains at $n<9$ are naturally self-avoiding. When $n \geq 9$, contact between beads on a single chain becomes possible. Depending on the flow conditions, chains adopt various conformations (Fig. 2). In fact, longer chains are more likely to form loops and various chain configurations.

In Fig. 5, we also plot the probability density function of the dimensionless end-to-end distance $x=r/L$, with r as the instantaneous end-end distance of a single chain and L as the relevant maximum contour length. For random walks, the distribution of end-to-end distance tends to follow a Gaussian curve as the number of beads becomes large [7,21]. In Fig. 5, we note that agreement with the Gaussian distribution increases as the number of beads increases. This effect is
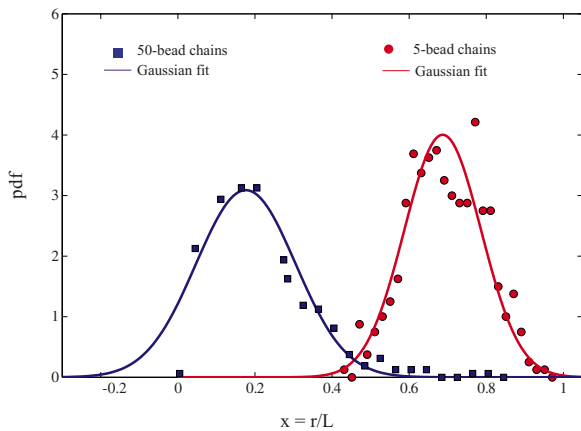
FIG. 5. (Color online) Probability density function of dimensionless end-to-end distance $x = r/L$ scaled by the maximum contour length L at rotation speed of 0.1 rev/s and 20% filling percentage. The solid lines show fits to Gaussian distribution curves, $pdf(x) = \exp(-(x-\mu)^2/2\sigma^2)/\sigma\sqrt{2\pi}$. For five-bead chains, $\mu = 0.69$ and $\sigma = 0.11$. For 50-bead chains, $\mu = 0.13$ and $\sigma = 0.12$.

consistent with the behavior of polymer melts, where the presence of other chains makes a long chain exhibit RW instead of SAW behavior.

Despite the short chain lengths ($5 \le n \le 50$) considered in our experiments, measured values of $\langle r^2 \rangle$ lie between 2D SAW and 2D RW and the power-law scaling provides a reasonable description [see Fig. 4(b)]. It is well known that the critical exponents ν become evident for walks of modest length ($n = 9$) for the 2D case, as evidenced by computer simulations [14,22–25], even though in principle the exponents are asymptotic values found for walks involving a very large number of beads (n).

Regarding the manifestation of the crossover transition occurring around $n = 9$, we know that for $n \ge 9$ the chains must elongate to form a loop. As the chain length increases, both intrachain and interchain interactions intensify. This trend leads to a crossover transition from 2D SAW to 2D RW behavior which occurs at around $n = 9$.

For $n < 9$, beads on each single chain are self-avoiding by default, while for longer chains the successive beads that do not form loops are usually in contact. Moreover, the longer the chain is, the more likely it is for two successive beads to be in contact so that excluded volume effects decrease. Longer chains therefore tend to follow a random-walk pattern. That is, with increasing link number N, $\langle r^2 \rangle$ falls closer to the RW trend line.

In summary, we have studied the dynamical and statistical behavior of flowing collection of granular chains confined within a 2D rotating tumbler. The length of the fully stretched chain is shorter than or comparable to the diameter of the two-dimensional tumbler. We found that: (a) Systems of granular chains display complicated packing and flow behavior when rotated in a 2D tumbler with axis perpendicular to gravity. (b) The average packing porosity increases with increasing rotation rate and decreasing filling percentage, partially due to the gravitational effect. The porosity also displays a jump at $n = 9$, the minimum bead number required to form the smallest loop of a single chain. (c) The statistical behavior of $\langle r^2 \rangle$ of a randomly selected chain during flow follows a crossover transition between 2D SAW to 2D RW behavior. Our results elucidate important statistical information of chain systems at macroscopic length scales. Future experiments will focus on the intrachain interactions and segregation behavior in systems of granular chains with different lengths.

[1] E. Ben-Naim, Z. A. Daya, P. Vorobieff, and R. E. Ecke, Phys. Rev. Lett. **86**, 1414 (2001).

[2] J. Hickford, R. Jones, S. C. du Pont, and J. Eggers, Phys. Rev. E **74**, 052101 (2006).

[3] M. B. Hastings, Z. A. Daya, E. Ben-Naim, and R. E. Ecke, Phys. Rev. E **66**, 025102(R) (2002).

[4] R. E. Ecke, Z. A. Daya, M. K. Rivera, and E. Ben-Naim, Mater. Res. Soc. Symp. Proc. **759**, 129 (2003).

[5] A. Belmonte, M. J. Shelley, S. T. Eldakar, and C. H. Wiggins, Phys. Rev. Lett. **87**, 114301 (2001).

[6] A. Kudrolli, G. Lumay, D. Volfson, and L. S. Tsimring, Phys. Rev. Lett. **100**, 058001 (2008).

[7] J. J. Prentis and D. R. Sisan, Phys. Rev. E **65**, 031306 (2002).

[8] R. B. Bird, *Dynamics of Polymeric Liquids* (Wiley, New York, 1987).

[9] B. Nienhuis, Phys. Rev. Lett. **49**, 1062 (1982).

[10] P. G. de Gennes, *Scaling Concepts in Polymer Physics* (Cornell University, Ithaca, 1979).

[11] C. Vanderzande, *Lattice Models of Polymers* (Cambridge University Press, New York, 1998).

[12] K. Kelly, D. L. Hunter, and N. Jan, J. Phys. A **20**, 5029 (1987).

[13] Y. Li and W. A. Goddard, J. Phys. Chem. B **110**, 18134 (2006).

[14] B. D. Hughes, *Random Walks and Random Environments* (Clarendon Press, New York, 1995).

[15] B. Maier and J. O. Rädler, Phys. Rev. Lett. **82**, 1911 (1999).

[16] F. Valle, M. Favre, P. De Los Rios, A. Rosa, and G. Dietler, Phys. Rev. Lett. **95**, 158105 (2005).

[17] J. M. Ottino and D. V. Khakhar, Annu. Rev. Fluid Mech. **32**, 55 (2000).

[18] J. Rajchenbach, Phys. Rev. Lett. **65**, 2221 (1990).

[19] See EPAPS Document No. E-PLEEE8-80-R18908 for a movie of the flow in the tumbler. For more information on EPAPS, see http://www.aip.org/pubservs/epaps.html.

[20] F. Kühner, M. Erdmann, and H. E. Gaub, Phys. Rev. Lett. **97**, 218301 (2006).

[21] M. Bishop and J. H. R. Clarke, J. Chem. Phys. **94**, 3936 (1991).

[22] A. J. Guttmann, J. Phys. A **20**, 1839 (1987).

[23] P. Grassberger, Z. Phys. B **48**, 255 (1982).

[24] C. Domb, J. Chem. Phys. **38**, 2957 (1963).

[25] J. L. Martin and M. G. Watts, J. Phys. A **4**, 456 (1971).